Journal of Advanced Research in Power Electronics & Power Systems
Volume 6, Issue 1&2 - 2019, Pg. No. 4-10
Peer Reviewed Journal

Research Article

# Implementation of an Inverter using a New SVPWM Technique

Gautam Moni Patro[1], Pasumarthi Mallikarjuna Rao[2]

[1,2]Department of Electrical Engineering, Andhra University, Visakhapatnam.

**I N F O**

**Corresponding Author:**
Gautam Moni Patro, Department of Electrical Engineering, Andhra University, Visakhapatnam.
**E-mail Id:**
gautammp@yahoo.co.in
**Orcid Id:**
https://orcid.org/0000-0003-3790-2852

**How to cite this article:**
Patro GM, Rao PM. Implementation of an Inverter using a New SVPWM Technique. *J Adv Res Power Electro Power Sys* 2019; 6(1&2): 4-10.

Date of Submission: 2019-12-05
Date of Acceptance: 2019-12-17

**A B S T R A C T**

Space Vector Modulation (SVPWM) is one of the most preferred Pulse Width Modulation(PWM) strategies. This form of scheme in Voltage Source Inverter (VSI) drives provides better use of bus voltage and less loss in commutation. Controlling three-phase inverter voltage by space-vector modulation involves switching between the two active and zero voltage vectors so that the time interval times the voltages in the chosen sectors is equal to the command voltage times the time period within each switching cycle. The reference voltage is presumed to be constant during the switching cycle as the time period would be very small. The SVPWM scheme can be easily implemented by simple digital measurement of the switching time. In this paper, three element sorting algorithm is used to calculate the switching times. The hardware is realized using DSPIC30F6010 microcontroller and tested using a resistive load.

**Keywords:** Space Vector PWM, Voltage Source Inverter, DSPIC30F6010, Three Element Sorting Algorithm

## Introduction

With advances in solid-state power electronic devices and microprocessors, various inverter control techniques employing Pulse Width Modulation (PWM) are becoming increasingly popular in AC motor drive applications. These PWM-based drives are used to control both the frequency and the magnitude of the voltages applied to motors. Various PWM strategies, control schemes, and realization techniques have been developed in the past two decades. PWM strategy plays an important role in the minimization of harmonics and switching losses in converters, especially in three-phase applications.

In the mid-1980s, SVPWM was first proposed by Van Der Broeck. By the year 1988 he significantly advanced the concept. In the present work, the Mathematical Three Element sorting algorithm model of three phase SVPWM is derived step by step and when compared it has similar results but the method of implementation is completely different. With the advancement of microprocessors, SVPWM has become one of the most significant PWM methods for three-phase inverters. The inverter hardware is developed/ implemented using the microcontroller DSPIC30F6010. The functionality of the inverter is tested using a resistive load and the complete timing sequences of the hardware used is checked with developed Simulation model.

In this paper, the work done is classified under following subsections as derivation of concept of SVPWM technique, three element sorting algorithm, Mathematical model of SVPWM Inverter and Hardware Implementation with Results.

## Mathematical Modelling of SVPWM Technique

Revolving MMF's in 3-phase machines are the three phase sinusoidal voltages fed to 3-phase windings and are produced in the air gap of a machine and are an example of space vector.

Pulsating magnetic field produced by single phase winding

$$Fr1=K*ir*\cos(\theta ae) \quad (1)$$

Where: - Fr1 = Fundamental part of MMF

θae=Electrical angle

$$Ir=Im*\cos(\omega e*t) \quad (2)$$

$$Fr1 = K*Im*\cos(\omega e*t)*\cos(\theta ae)$$

$$= (F(max/2))*[\cos(\theta ae-\omega et) + \cos(\theta ae+\omega et)]\ Fr1 \quad (3)$$

$$Fr1 = Fr(+) + Fr(-) \quad (4)$$

Where: -

K = Constant related to winding distribution factor

F(max) = Maximum value of mmf

Ir = current flowing through ‘r’ phase

Pulsating magnetic field can be resolved into two revolving magnetic field components, one rotating clockwise and other rotating anticlockwise.

3-phase windings excited by 3-phase sinusoidal currents in an AC machine:

$$ir = Im*\cos(\omega et) \quad (5)$$

$$iy = Im*\cos(\omega et-120°) \quad (6)$$

$$ib = Im*\cos(\omega et+120°) \quad (7)$$

Revolving magnetic field:

$$Fr1 = K*ir*\cos(\theta ae) \quad (8)$$

$$Fy1 = K*iy*\cos(\theta ae-120°) \quad (9)$$

$$Fb1 = K*ib*\cos(\theta ae-240°) \quad (10)$$

$$Fr1 = Fmax*\cos(\theta ae)*\cos(\omega et) \quad (11)$$

$$Fy1 = Fmax*\cos(\theta ae-120°)*\cos(\omega et-120°) \quad (12)$$

$$Fb1 = Fmax*\cos(\theta ae-240°)*\cos(\omega et-240°) \quad (13)$$

$$Fr1=\frac{Fmax}{2[\cos(\theta ae-\omega et)+\cos(\theta ae+\omega et)]} \quad (14)$$

$$Fy1=\frac{Fmax}{2[\cos(\theta ae-\omega et)+\cos(\theta ae+\omega et+120°)]} \quad (15)$$

$$Fb1=\frac{Fmax}{2[\cos(\theta ae-\omega et)+\cos(\theta ae+\omega et+240°)]} \quad (16)$$

$$Fag1=(Fr(+)+Fy(+)+Fb(+))+(Fr(-)+fy(-)+Fb(-)) \quad (17)$$

$$Favg1 = (3*Fmax/2)*\cos(\theta ae-\omega et) \quad (18)$$

Equivalent Two-phase Windings: Revolving MMF’s can be produced by equivalent two-phase windings. The two-phase winding axes are separated by 90° degrees and excited by currents which are phase shifted by 90° in time.

Equivalence of 3-phase and two-phase windings:

$$N*i\alpha = N*ir+N*iy*\cos 120°+N*ib*\cos 240° \quad (19)$$

$$N*i\beta = N*iy*\sin 120°+N*ib*\sin 240° \quad (20)$$

$$i\alpha = ir + iy*\cos 120° + ib*\cos 240° \quad (21)$$

$$i\alpha = ir - (iy/2) - (ib/2)=3/2*ir \quad (22)$$

(since) $ir+ iy+ ib = 0$

$$i\beta = iy*\sin 120° + ib*\sin 240° = (\sqrt{3}/2)*(iy-ib) \quad (23)$$

$$i\beta = (\sqrt{3}/2)*(iy-ib) \quad (24)$$

$$\begin{bmatrix} i\alpha \\ i\beta \end{bmatrix} = \begin{bmatrix} \frac{3}{2} & 0 & 0 \\ 0 & \frac{\sqrt{3}}{2} & \frac{-\sqrt{3}}{2} \end{bmatrix} * \begin{bmatrix} ir \\ iy \\ ib \end{bmatrix} \quad (25)$$

where iα, iβ are two phase currents derived from the phase currents (ir, iy, ib) of the three phase system, and N=Number of turns.

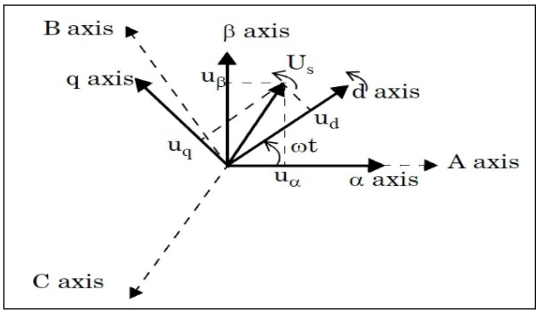


**Figure 1.Representing 3-Phase to Two Phase and dq-axes Conversion**

Similarly, for 3-phase voltages with balanced star connected load

$$V\alpha= (3/2)*Vrn \quad (26)$$

$$V\beta= ((\sqrt{3})/2)*(Vyn- Vbn) \quad (27)$$

$$ir + iy + ib = 0 \quad (28)$$

$$Vrn + Vyn + Vbn = 0 \quad (29)$$

Similar to equation of plane x+y+z = 0

A plane has only 2 dimensions.

Three phase quantities sum up to zero and hence can be represented by only two independent quantities.

## Svpwm for a 2 Level Inverter

Voltage vectors in terms of 3-phase pole voltages:

$$Vro = \pm 0.5Vdc \quad (30)$$

$$Vyo = \pm 0.5Vdc \quad (31)$$

$$Vbo = \pm 0.5Vdc \quad (32)$$

$$V\alpha = (3/2)*Vrn \quad (33)$$

$$V\alpha = (1/2)*(Vry-Vbr) \quad (34)$$

$$V\alpha = (1/2)*(Vro-Vyo-Vbo) \quad (35)$$

$$V\beta = ((\sqrt{3})/2)*(Vyn-Vbn) \quad (36)$$

$$V\beta = ((\sqrt{3})/2)*(Vyo-Vbo) \quad (37)$$

Where:-

Vdc is DC bus voltage

$V\alpha$ , $V\beta$ are Two phase voltages

Vrn, Vyn, Vbn are Three phase voltages

Vro,Vyo,Vbo are Pole voltage of the inverter

The tip of the voltage space vector follows a circular trajectory with maximum magnitude of $(\sqrt{3}/2)*Vdc$. The rotating reference space vector is samples at a high sampling frequency of (Ts).

Zero period (To) = $Ts-(T1+T2)$ (38)

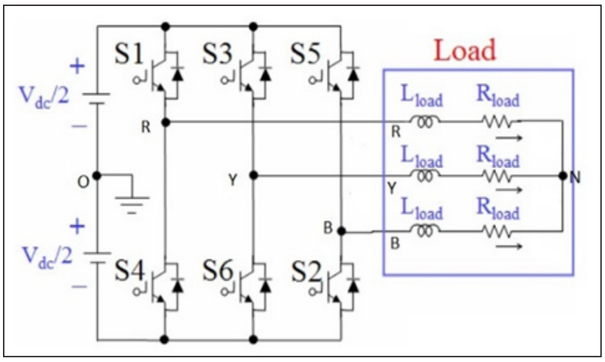


**Figure 2.Two Level Voltage Source Inverter with 3-phase Balanced Load and Un-connected Neutral**

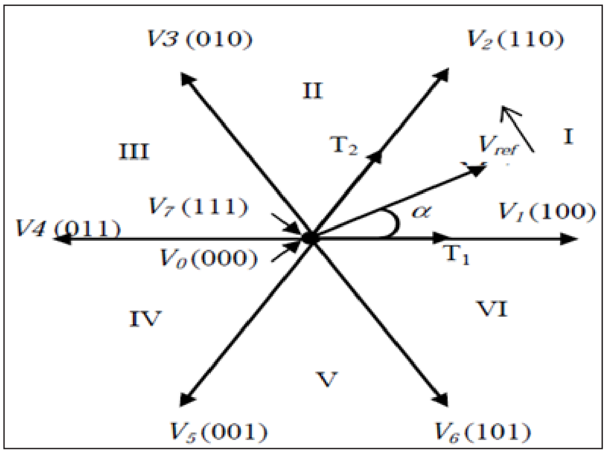


**Figure 3.Inverter States and Voltage Vectors of a 2 Level Voltage Source Inverter**

The volt sec along $\alpha$ axis i.e along V1 axis

$(V1*T1) + (V2*\cos(60°)*T2) = |Vs|*Ts*\cos(\alpha)$ (39)

Volt sec along $\beta$ axis which is perpendicular to $\alpha$ axis:

$0 + (V2*\sin(60°))* T2 = |Vs|* Ts* \sin(\alpha)$ (40)

Volt sec along $\beta$ axis which is perpendicular to $\alpha$ axis:

$0 + (V2*\sin (60°))*T2 = |Vs|*Ts*\sin(\alpha)$ (41)

By considering $|V1|= |V2| = Vdc$ and solving for T1 and T2

$T1 = Ts* (|Vs|/Vdc)*(\sin (60°-\alpha)/\sin (60°))$ (42)

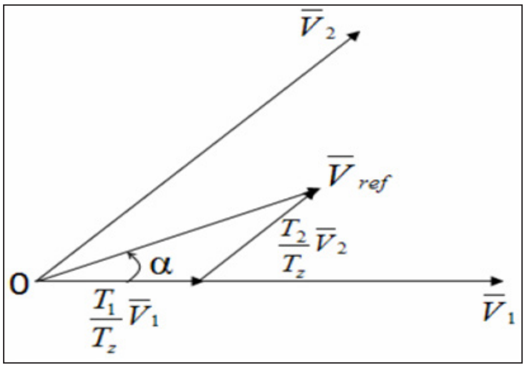


**Figure 4.Inverter States and Voltage Vectors (Sector I) of a 2 Level Voltage source Inverter**

$T1 = (2/\sqrt{3})*Ts*(Vs/Vdc)*\sin (60°-\alpha)$ (43)

$T2 = Ts* (|Vs|/Vdc)*((\sin(\alpha)/\sin(60°))$ (44)

$T2 = (2/\sqrt{3})*Ts*(Vs/Vdc)*\sin(\alpha)$ (45)

In sector 1 for $0< \alpha < 60$

Zero period (To) = $Ts-(T1+T2)$ (46)

Minimum switching is to be ensured in order to achieve low losses.

Switching time duration in any sector is given by:

$T1 = \sqrt{3}*Tz*(|Vref|/Vdc)*(\sin(60°-\alpha+((n-1)/3*Pi))$ (47)

$T1 = \sqrt{3}*Tz*(|Vref|/Vdc)*(\sin(n/3*pi-\alpha)$ (48)

$T1 = \sqrt{3}*Tz*(|Vref|/Vdc)*(\sin(n/3*pi)*\cos(\alpha)$

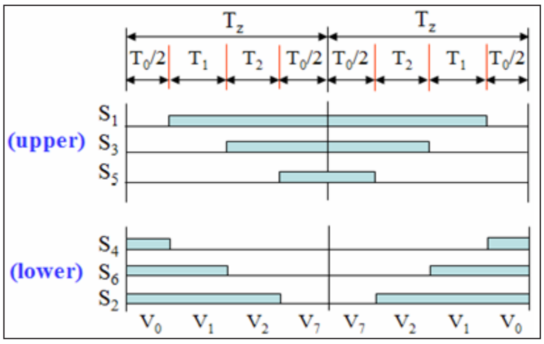


**Figure 5.Switching Pattern in Sector I**

$-\cos(n/3*pi)*\sin\alpha)$ (49)

$T2 = \sqrt{3}*Tz*(|Vref|/Vdc)*(\sin(\alpha-((n-1)/3)*pi))$ (50)

$T2 = \sqrt{3}*Tz*(|Vref|/Vdc)*(-\cos(\alpha)*\sin((n-1)/3*pi)$

$+\sin(\alpha)*\cos((n-1)/3*pi)$ (51)

$To = Tz-T1-T2$ (52)

Where Tz = Ts (Sampling times), n=Sector number.

$Vro(avg) = ((Vdc/2)/Ts)*(-To/2+T1+T2+To/2)$ (53)

$Vro(avg) = ((Vdc/2)/Ts)*(T1+T2)$ (54)

$Vyo(avg) = ((Vdc/2)/Ts)* (-To/2-T1+T2+To/2)$ (55)

$Vyo(avg) = ((Vdc/2)/Ts)*(-T1+T2)$ (56)

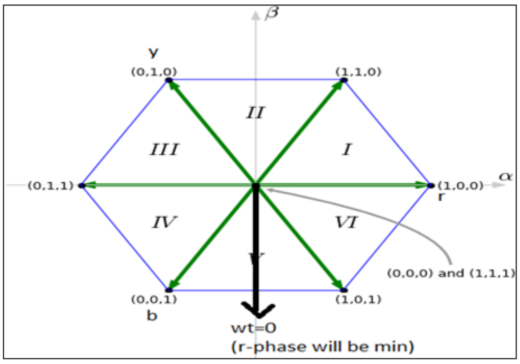


**Figure 6.Switching Pattern in Sector I**

$V_{bo}(avg) = ((V_{dc}/2)/T_s)*(-T_o/2-T1-T2+T_o/2)$ (57)

$V_{bo}(avg) = ((V_{dc}/2)/T_s)*(-T1-T2)$ (58)

$V_{bo}(avg) = -V_{ro}(avg)$ (59)

Already the values of T1 and T2 in sector 1 are there for substituting in above equations. Now average voltages are

$V_{ro}(avg) = ((V_{dc}/2)/T_s)*[T_s*(|V_s|/V_{dc})$

$*(2/\sqrt{3})*\sin(60°-\alpha) + T_s*(|V_s|/V_{dc})$

$*(2/\sqrt{3})*T_s*(|V_s|/V_{dc})*(2/\sqrt{3})*\sin\alpha]$ (60)

$V_{ro}(avg) = |V_s|/\sqrt{3}*\sin(60°+\alpha)$ (61)

$V_{yo}(avg) = ((V_{dc}/2)/T_s)*[-T_s*(|V_s|/V_{dc})*(2/\sqrt{3})$

$*\sin(60°-\alpha)+T_s*(|V_s|/V_{dc})*(2/\sqrt{3})$

$*T_s*(|V_s|/V_{dc})*(2/\sqrt{3})*\sin\alpha]$ (62)

$V_{yo}(avg) = |V_s|*\sin(\alpha-30°)$ (63)

Average variation of phase R (pole-R) i.e Vro(avg) for a cycle of operation in sector 5 for 0≤wt≤30° (middle of sector-5 to end of sector-5)

The Vro(avg) is the same as Vyo(avg) in sector 1 as from (0 to 1)

$V_{ro}(avg) = |V_s|\sin(\alpha-30°)$ (64)

Now we replace α by wt

$V_{ro}(avg) = |V_s|\sin(wt+30°-30°)$ (65)

$V_{ro}(avg) = |V_s|\sin(wt)$ (66)

only for 0≤wt≤30°

When wt varies from 30° to 90° (30°≤wt≤90°) in sector 6 the variation of switch is from 1 to 1 so it is same as in sector 1. So Vro(avg) is also same.

$V_{ro}(avg) = (|V_s|/\sqrt{3})*\sin(\alpha)$ (67)

0≤α≤60°, 30°≤wt≤90°

$V_{ro}(avg) = (|V_s|/\sqrt{3})*\sin(wt+30°)$ (68)

as α=wt+30°

Space vector pwm using only the sampled reference phase amplitude

$T1 = \sqrt{3}*T_z*(|V_{ref}|/V_{dc})*(\sin(n/3*pi-\alpha))$ (69)

$T2 = (2/\sqrt{3})*T_s*(V_s/V_{dc})*\sin(\alpha)$ (70)

$V\alpha = (3/2)*V_{rn}$ (71)

$V\beta = (\sqrt{3}/2)*(V_{yn}-V_{bn})$ (72)

In sector -1

$T1 = (2/\sqrt{3})*(T_s/V_{dc})*[|V_s|*\cos(\alpha)*\sin(60°)$

$-|V_s|*\sin(\alpha)*\cos(60°)|]$ (73)

As ($|V_s|*\cos(\alpha) = V\alpha$ and $V\alpha=(3/2)*V_r*\sin(60°)$)

Also ($|V_s|*\sin\alpha=V\beta$) and

$V\beta = (\sqrt{3}/2)*(V_y-V_b)*\cos(60°)$ (74)

$V\beta = (T_s/V_{dc})*[(3/2)*V_r-(1/2)*V_y+(1/2)*V_b]$ (75)

$V\beta = (T_s/V_{dc})*[V_r-V_y]$ (76)

$V\beta = T_s(V_r/V_{dc})-T_s(V_y/V_{dc})$ (77)

$V\beta = T_{rs}-T_{ys}$ (78)

$T2 = (2/\sqrt{3})*(|V_s|/V_{dc})*T_s*\sin(\alpha)$ (79)

$T2 = (2/\sqrt{3})*(T_s/V_{dc})*V\beta$ (80)

$T2 = (2/\sqrt{3})*(T_s/V_{dc})*(\sqrt{3}/2)*(V_y-V_b)$ (81)

$T2 = (T_s/V_{dc})*[V_y-V_b]$ (82)

$T2 = T_{ys}-T_{bs}$ (83)

In sector-2

$T1 = (2/\sqrt{3})*(T_s/V_{dc})*[(V\alpha*\cos 90° + V\beta*\cos 30°)$

$-(-V\alpha*\cos 30°+V\beta*\cos 60°)*\cos(60°)]$ (84)

$T1 = (2/\sqrt{3})*(V_y/2-V_b/2+(3/2)*V_r)$ (85)

$T1 = T_s/V_{dc}(V_r-V_b)$ (86)

$T1 = T_{rs}-T_{bs}$ (87)

$T2 = T_{ys}-T_{rs}$ (88)

Similarly, the values of T1 & T2 in other sectors are derived and the summary of the results are given in table below.

**Table 1.T1&T2 Values in all the Six Sectors**

| Sector | (To/2) | T1 | T2 |
|---|---|---|---|
| 1 | $(T_s-T_{rs}+T_{bs})/2$ | $T_{rs}-T_{ys}$ | $T_{ys}-T_{bs}$ |
| 2 | $(T_s+T_{bs}-T_{ys})/2$ | $T_{rs}-T_{bs}$ | $T_{ys}-T_{rs}$ |
| 3 | $(T_s+T_{rs}-T_{ys})/2$ | $T_{ys}-T_{bs}$ | $T_{bs}-T_{rs}$ |
| 4 | $(T_s+T_{rs}-T_{bs})/2$ | $T_{ys}-T_{rs}$ | $T_{bs}-T_{ys}$ |
| 5 | $(T_s+T_{ys}-T_{bs})/2$ | $T_{bs}-T_{rs}$ | $T_{rs}-T_{ys}$ |
| 6 | $(T_s+T_{ys}-T_{rs})/2$ | $T_{bs}-T_{ys}$ | $T_{rs}-T_{bs}$ |

## Element Sorting Algorithm for Space Vector Modulation

The algorithm is defined by the following steps:

Step 1: First considering the 3-phase voltages (Vr, Vy, Vb), sampling time (Ts) and dc bus voltage (Vdc). Where

$$Vr+Vy+Vb=0 \tag{89}$$

Step 2: Finding the sampled reference phase amplitude

$$Trs=Ts*(Vr/Vdc) \tag{90}$$

$$Tys=Ts*(Vy/Vdc) \tag{91}$$

$$Tbs=Ts*(Vb/Vdc) \tag{92}$$

Step 3: ConsideringTmax=Trs and Tmin=Trs

$$if(Tys>Tmax) \rightarrow Tmax=Tys \tag{93}$$

$$if(Tys<Tmin) \rightarrow Tmin=Tys \tag{94}$$

$$if(Tbs>Tmax) \rightarrow Tmax=Tbs \tag{95}$$

$$if(Tbs<Tmin) \rightarrow Tmin=Tbs \tag{96}$$

Step 4: Effective time calculation

$$Teff=Tmax-Tmin \tag{97}$$

$$Tzero = Tsample- Teff \tag{98}$$

$$Toffset=Tzero/2 – Tmin \tag{99}$$

Step 5: Gating signals in a sampling period during which top switch in a leg is latched ON

$$Tgr=Trs+Toffset \tag{100}$$

$$Tgy=Tys+Toffset \tag{101}$$

$$Tgb=Tbs+Toffset \tag{102}$$

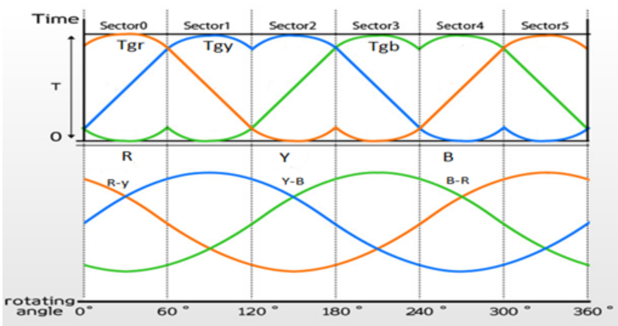


**Figure 7.Figure Representing Gating Times Tgr, Tgy, Tgb and Input Reference Voltages Vr, Vy, Vb**

## Advantages of this SVPWM Algorithm

There is no requirement for a look up table. The need for Sector identification and angle ‘α’ information is eliminated. Voltage space vector amplitude measurement is also not wanted. Only sampled reference space amplitudes in a sampling period are desirable. Extra boosting can be achieved when compared to sine PWM. This is because (a) due to presence of 3n content & flat area of sine wave is increasing. (b) in sine PWM the zero vector periods are not equal during sampling period Ts.

When we consider Vs is along Vα

$$V\alpha(max) = Vdc(\sqrt{3}/2) \tag{103}$$

$$V\alpha = Vr+Vy*\cos(120°) + Vb*\cos(240°) \tag{104}$$

$$V\alpha = Vr-(1/2)*(Vy+Vb) \tag{105}$$

$$V\alpha = (3/2)*Vr \tag{106}$$

$$Vr = V\alpha*(2/3) \tag{107}$$

$$Vr(max) = V\alpha(max)*(2/3) \tag{108}$$

$$Vr(max) = Vdc/(\sqrt{3})=0.577Vdc \tag{109}$$

## Simulation Model

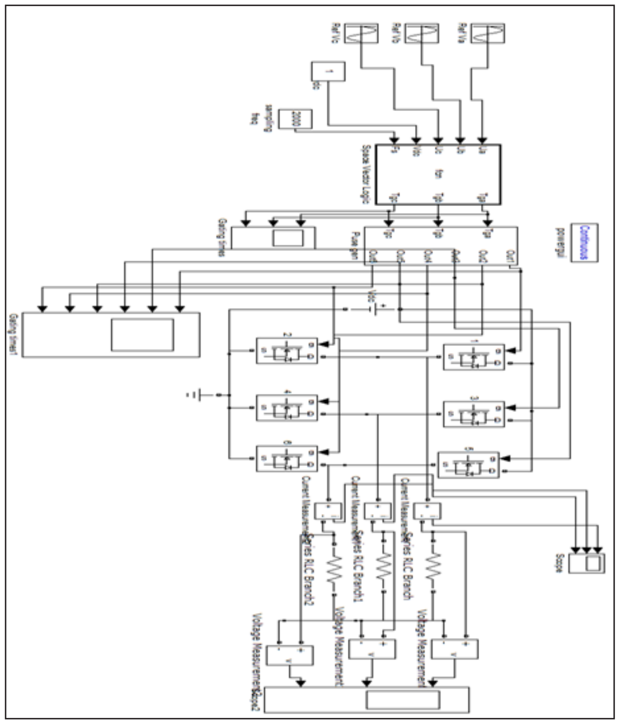

**Figure 8.Simulation Diagram of AFPMSM**

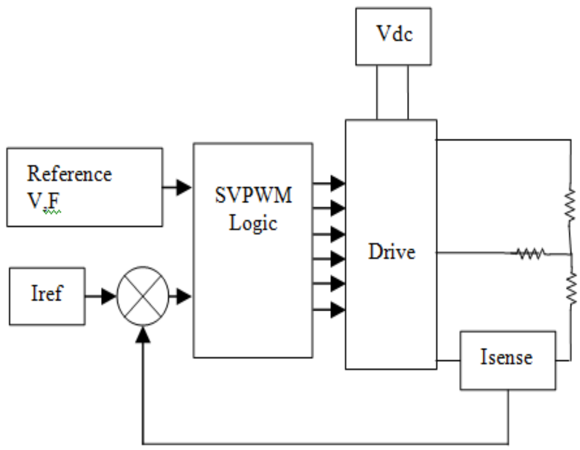


**Figure 9.Block Diagram of AFPMSM**

The Simulation of SVPWM Inverter using three element sorting algorithm is done. The adapted simulation environment is high flexible and expandable which allows the possibility of development of a set of functions for a detailed analysis of the Inverter.

The functional block diagram of the system is designed as shown in the figure 9.

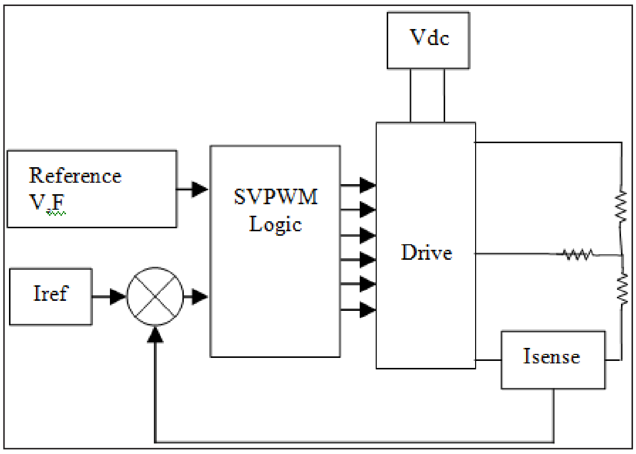


**Figure 9.Block Diagram of AFPMSM**

The advantageous features of the method are well shown in the following results:

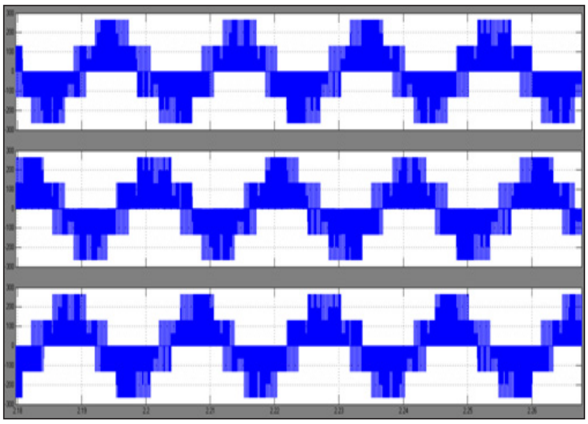

**Figure 10.Three phase Output Voltage Waveforms of SVPWM Inverter which are applied to AFPMSM Motor Model.(X-axis Represents Time; Y-axis Represents Voltage-(max Value is 266 Volts))**

## Experiment Setup

The hardware model of SVPWM Inverter using 3-Element sorting algorithm is realized using DSPIC30F6010 Microcontroller.

- Some of the components used for realization are:
- DSPIC30F6010 Microcontroller of Microchip make.
- High Speed MOSFET Driver IR2110
- Isolator IC – PC817
- MOSFET bridge circuit using IRF540

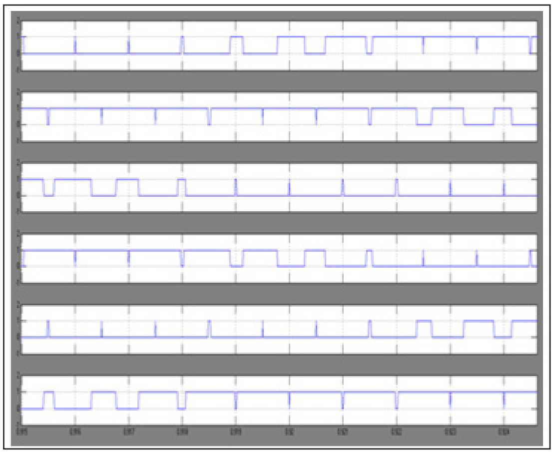

**Figure 11.Switching Pattern of the Six PWM Wave Forms**

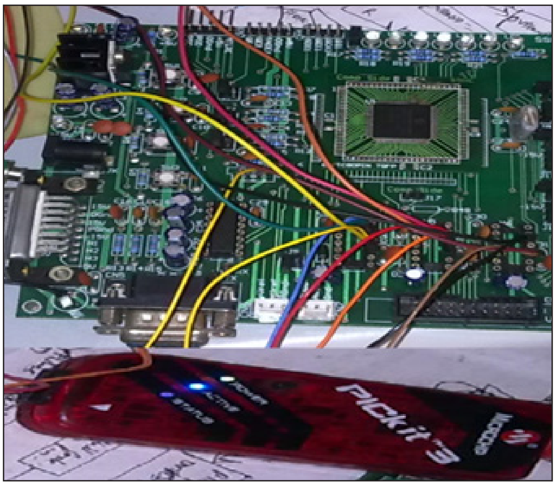


**Figure 12.Micro controller on PCB & Programmer PICKit 3**

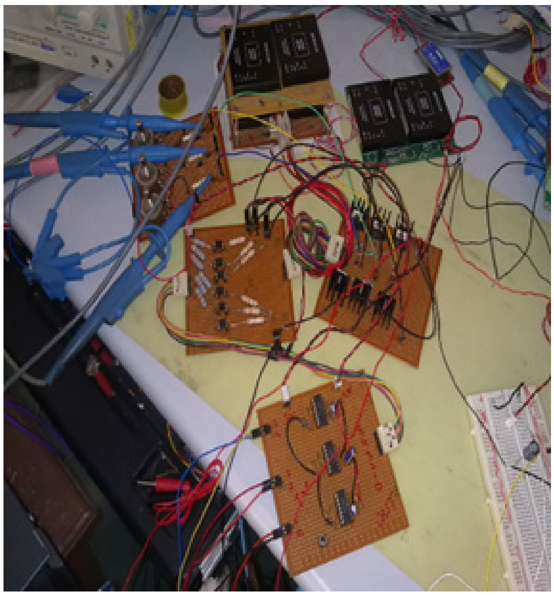

**Figure 13.Setup for Hardware implementation of Inverter**

The hardware is tested with:

- Resistive load of 2KOhms.
- Reference wave frequency of 50Hz.
- Vdc applied to bridge is 30Volts.
- PWM frequency is considered at 2000 hertz.

## Results of Hardware Implementation

The results taken with a Modulation Index of 100% i.e with Reference wave amplitude of 0.577.

The results taken with a Modulation Index of 86.65% i.e with Reference wave amplitude of 0.5 and Vdc reference = 1.

## Conclusion

The results obtained from the hardware implementation fall in line with the results obtained from simulation and are reported. The ripple magnitude of output voltage is being reduced by increasing the PWM frequency or adding filters across output. As the Modulation Index is increased the RMS value of the output voltage correspondingly raises. At different modulation indexes the better output voltages can be obtained at nearly 80%.

An easier and less complex technique for SVPWM logic is presented using the three element algorithm. Due to the simplicity of the algorithm, it is further be extended/used in the digital implementation of SVPWM using a suitable microcontroller.. In the implementation of this hardware the major difficulties that came through are the Micro controller speed limitation and internal timer setting for generation of reference waves at 50 Hz frequency. The problem of controller speed limitation could be resolved to some extent by using a DSPIC30F6010 processor of Microchip make and running it with an external crystal of 40 MHz.

## References

1. Heydari F et al. Predictive field-oriented control of PMSM with space vector modulation technique. *Frontiers of Electrical and Electronic Engineering in China* 2010; 5(1): 91-99.
2. Kanchan RS, Baiju MR, Mohapatra KK, Ouseph PP, Gopakumar K. Space vector PWM signal generation for multilevel inverters using only the sampled amplitudes of reference phase voltages. *IEE Proceedings-Electric Power Applications* 2005; 152(2): 297-309.
3. Min RH, Kim JH, Sul SK. Analysis of multiphase space vector pulse-width modulation based on multiple dq spaces concept. *IEEE Transactions on Power Electronics* 2005; 20(6): 1364-1371.
4. Pillay P, Krishnan R. Development of digital models for a vector controlled permanent magnet synchronous motor drive. Conference Record IEEE Industry Applications Society Annual Meeting 1988; 14(6): 476-482.
5. Pillay P, Krishnan R. Modeling, Simulation and analysis of permanent-magnet motor drives I. The permanent-magnet synchronous motor drive. *IEEE Transactions on Industry Applications* 1989; 5(2): 265-273.
6. Pillay P, Krishnan R. Control characteristics and speed controller design for a high performance permanent magnet synchronous motor drive. *IEEE Transactions on Power Electronics* 1990; 5(2): 151-159.
7. Hwan O, Jung SY, Youn MJ. A Source Voltage-Clamped Resonant Link Inverter for a PMSM Using a Predictive Current Control Technique. *IEEE Transactions on Power Electronics* 1999; 14(6): 1122-1132.
8. McGrath BP, Holmes DG, Lipo T. Optimized Space Vector Switching Sequences for Multilevel Inverters. *IEEE Transactions on Power Electronics* 2005; 18(6): 1293-1301.
9. Fasil MC, Antaloae N, Mijatovic B, Jensen B, Holboll J. Improved dq-Axes Model of PMSM Considering Airgap Flux Harmonics and Saturation. *IEEE Transactions on Applied Superconductivity* 2016; 26(4): 5202705.
10. Zhou C, Yang G, Jianyong S. PWM Strategy with Minimum Harmonic Distortion for Dual Three-Phase Permanent-Magnet Synchronous Motor Drives Operating in the Overmodulation Region. *IEEE Transactions on Power Electronics* 2016; 31(2): 1367-1380.
11. Karttunen J, Kallio S, Peltoniemi P, Silventoinen P, Pyrhonen O. Decoupled vector control scheme for dual three-phase permanent magnet synchronous machines. *IEEE Transactions on Industrial Electronics* 2014; 61(5): 2185-2196.
12. Qian J, Rahman MA. Analysis of Field Oriented Control for Permanent Magnet Hysteresis Synchronous Motors. *IEEE Transactions on Industrial Electronics* 1993; 29(6): 1156-1163.
13. Li B, Chen W. Comparative analysis on PMSM control system based on SPWM and SVPWM. IEEE Chinese Control and Decision Conference 2016: 5071-5075.
14. Zhou LQ. Dead-time Compensation Method of SVPWM Based on DSP. IEEE Conference on Industrial Electronics and Applications 2009: 2355-2358.
15. Moon HT, Kim HS, Youn MJ. A Discrete-Time Predictive Current Control for PMSM," *IEEE Transactions on Power Electronics* 2003; 18(1): 464-472.